

1,4-Cyclohexanedione–Bromate–Acid Oscillatory System. IV. Reduced Models

István Szalai, Endre Körös,* and László Györgyi

Department of Inorganic and Analytical Chemistry, L. Eötvös University,
1518 Budapest, P.O. Box 32, Hungary

Received: August 4, 1998

A 27-reaction, 15-species mechanistic model of the oscillatory 1,4-cyclohexanedione (CHD)–bromate–acid system recently introduced by Szalai and Körös is analyzed. Both the important reactions and major interactions are identified using the principal component analysis. These considerations result in a 21-reaction, 14-species reduced mechanism that reproduces the behavior of the original model. This model is further simplified to a three-variable (HBrO_2 , Br^- , and H_2Q) skeleton model that differs from the Oregonator model. For, it attributes an essential role to H_2Q (1,4-dihydroxybenzene), a species continuously generated in the redox reaction of CHD and bromate. It is shown that the CHD–bromate reacting system is closely related dynamically to the “emptying/refilling” CSTR oscillators.

Introduction

We have examined the behavior of the 1,4-cyclohexanedione (CHD)–bromate–acid uncatalyzed bromate oscillator (UBO) in a recent sequence of papers^{1,2} and suggested a detailed chemical mechanism (Table 1). Our proposed mechanism composed of 27 steps includes both the purely inorganic reactions (oxybromine chemistry) and those involving organic species. Its essence is based on the experimentally verified finding that CHD in its reaction with acidic bromate gives 1,4-dihydroxybenzene (H_2Q), which plays a key role in the oscillatory reaction (Figure 1). The reaction of H_2Q and bromate shows a Landolt (clock)-type dynamics, and the presence of CHD converts the reacting system into an oscillatory one. An analogy between this system and the oscillatory Landolt reactions³ [e.g. $\text{IO}_3^- - \text{SO}_3^{2-} - \text{Fe}(\text{CN})_6^{4-}$] was claimed.

Here we report construction of a reduced model (of skeleton type) with the minimum number of dynamic variables that can describe oscillations in the CHD–bromate–acid system.

Analysis of the Model

Analysis of the mechanism was accomplished by principal component analysis of the rate-sensitivity matrix ($\partial \ln f_i(t)/\partial \ln k_j$) at particular times in a simulation. Principal component analysis requires the determination of the eigenvalues and eigenvectors of $\mathbf{F}^T \mathbf{F}$. The eigenvectors reveal strongly interacting reaction sequences, and the corresponding eigenvalues measure the significance of the separate parts of the mechanism. For a detailed description of this method we refer to the literature.⁴ It is possible by this method to identify both the important reactions and the major reaction interactions. We studied the model from the start of the oscillations. The time points of the analyses are shown in Figure 2.

We identified and analyzed the most important reaction clusters. One of these is the protonation equilibrium of HBrO_2 .



This fast equilibrium is established at all time points of the analysis. A quasi-steady-state assumption (QSSA) for H_2BrO_2^+

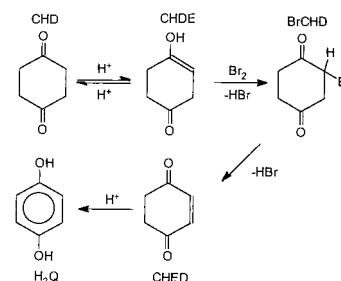


Figure 1. Mechanism of the formation of 1,4-dihydroxybenzene.

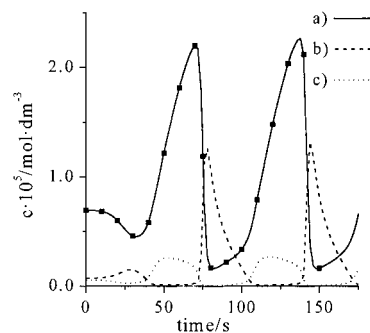
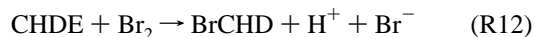


Figure 2. Time points of the sensitivity analysis. Initial concentrations: $[\text{CHD}]_0 = 0.0571 \text{ mol dm}^{-3}$, $[\text{NaBrO}_3]_0 = 0.0791 \text{ mol dm}^{-3}$, $[\text{BrCHD}]_0 = 0.0205 \text{ mol dm}^{-3}$, $[\text{CHED}]_0 = 0.00425 \text{ mol dm}^{-3}$, $[\text{Q}]_0 = 0.0182 \text{ mol dm}^{-3}$, $[\text{H}^+]_0 = 1.29 \text{ mol dm}^{-3}$. Lines are the simulated concentrations of (a) H_2Q , (b) HBrO_2 , and (c) Br^- .

connects this equilibrium to the disproportionation of $\text{Br}(\text{+III})$, i.e., to reaction R5.

Another important reaction cluster is the bromination of CHD (Figure 1):



Since CHD is in large excess and reaction R12 is very fast, bromine is consumed completely in this process during the oscillatory period.

TABLE 1: Mechanistic Model of the CHD–Bromate–Acid Oscillatory System^a

R1	$\text{Br}^- + \text{HOBr} + \text{H}^+ \rightleftharpoons \text{Br}_2 + \text{H}_2\text{O}$	$k_1 = 8 \times 10^9 \text{ mol}^{-2} \text{ dm}^6 \text{ s}^{-1}$	$k_{-1} = 80 \text{ s}^{-1}$
R2	$\text{Br}^- + \text{HBrO}_2 + \text{H}^+ \rightleftharpoons 2\text{HOBr}$	$k_2 = 2.5 \times 10^6 \text{ mol}^{-2} \text{ dm}^6 \text{ s}^{-1}$	$k_{-2} = 2 \times 10^{-5} \text{ mol}^{-1} \text{ dm}^3 \text{ s}^{-1}$
R3	$\text{Br}^- + \text{BrO}_3^- + 2\text{H}^+ \rightleftharpoons \text{HOBr} + \text{HBrO}_2$	$k_3 = 1.2 \text{ mol}^{-3} \text{ dm}^9 \text{ s}^{-1}$	$k_{-3} = 3.2 \text{ mol}^{-2} \text{ dm}^6 \text{ s}^{-1}$
R4	$\text{HBrO}_2 + \text{H}^+ \rightleftharpoons \text{H}_2\text{BrO}_2^+$	$k_4 = 2 \times 10^6 \text{ mol}^{-1} \text{ dm}^3 \text{ s}^{-1}$	$k_{-4} = 1 \times 10^8 \text{ s}^{-1}$
R5	$\text{HBrO}_2 + \text{H}_2\text{BrO}_2^+ \rightarrow \text{HOBr} + \text{BrO}_3^- + 2\text{H}^+$	$k_5 = 1.7 \times 10^5 \text{ mol}^{-1} \text{ dm}^3 \text{ s}^{-1}$	
R6	$\text{HBrO}_2 + \text{BrO}_3^- + \text{H}^+ \rightleftharpoons \text{Br}_2\text{O}_4 + \text{H}_2\text{O}$	$k_6 = 48 \text{ mol}^{-2} \text{ dm}^6 \text{ s}^{-1}$	$k_6 = 3.2 \times 10^3 \text{ s}^{-1}$
R7	$\text{Br}_2\text{O}_4 \rightleftharpoons 2\text{BrO}_2^*$	$k_7 = 7.5 \times 10^4 \text{ s}^{-1}$	$k_{-7} = 1.4 \times 10^9 \text{ mol}^{-1} \text{ dm}^3 \text{ s}^{-1}$
R8	$\text{H}_2\text{Q} + \text{BrO}_2^* \rightarrow \text{HQ}^* + \text{HBrO}_2$	$k_8 = 8 \times 10^5 \text{ mol}^{-1} \text{ dm}^3 \text{ s}^{-1}$	
R9	$\text{HQ}^* + \text{BrO}_2^* \rightarrow \text{Q} + \text{HBrO}_2$	$k_9 = 8 \times 10^9 \text{ mol}^{-1} \text{ dm}^3 \text{ s}^{-1}$	
R10	$2 \text{HQ}^* \rightleftharpoons \text{H}_2\text{Q} + \text{Q}$	$k_{10} = 8.8 \times 10^8 \text{ mol}^{-1} \text{ dm}^3 \text{ s}^{-1}$	$k_{-10} = 7.7 \times 10^{-4} \text{ mol}^{-1} \text{ dm}^3 \text{ s}^{-1}$
R11	$\text{CHD} + \text{H}^+ \rightleftharpoons \text{CHDE} + \text{H}^+$	$k_{11} = 2.13 \times 10^{-4} \text{ mol}^{-1} \text{ dm}^3 \text{ s}^{-1}$	$k_{-11} = 5.2 \times 10^2 \text{ mol}^{-1} \text{ dm}^3 \text{ s}^{-1}$
R12	$\text{CHDE} + \text{Br}_2 \rightarrow \text{BrCHD} + \text{H}^+ + \text{Br}^-$	$k_{12} = 2.8 \times 10^9 \text{ mol}^{-1} \text{ dm}^3 \text{ s}^{-1}$	
R13	$\text{CHDE} + \text{HOBr} \rightarrow \text{BrCHD} + \text{H}_2\text{O}$	$k_{13} = 2.8 \times 10^9 \text{ mol}^{-1} \text{ dm}^3 \text{ s}^{-1}$	
R14	$\text{BrCHD} \rightarrow \text{CHED} + \text{Br}^- + \text{H}^+$	$k_{14} = 5 \times 10^{-5} \text{ mol}^{-1} \text{ dm}^3 \text{ s}^{-1}$	
R15	$\text{CHED} + \text{H}^+ \rightarrow \text{H}_2\text{Q} + \text{H}^+$	$k_{15} = 1.94 \times 10^{-4} \text{ mol}^{-1} \text{ dm}^3 \text{ s}^{-1}$	
R16	$\text{H}_2\text{Q} + \text{Br}_2 \rightarrow \text{Q} + 2\text{Br}^- + 2\text{H}^+$	$k_{16} = 3 \times 10^4 \text{ mol}^{-1} \text{ dm}^3 \text{ s}^{-1}$	
R17	$\text{H}_2\text{Q} + \text{BrO}_3^- + \text{H}^+ \rightarrow \text{Q} + \text{HBrO}_2 + \text{H}_2\text{O}$	$k_{17} = 2 \times 10^{-2} \text{ mol}^{-2} \text{ dm}^6 \text{ s}^{-1}$	
R18	$\text{H}_2\text{Q} + \text{HOBr} \rightarrow \text{Q} + \text{Br}^- + \text{H}^+ + \text{H}_2\text{O}$	$k_{18} = 6 \times 10^5 \text{ mol}^{-1} \text{ dm}^3 \text{ s}^{-1}$	
R19	$\text{CHD} + \text{BrO}_3^- + \text{H}^+ \rightarrow \text{H}_2\text{Q} + \text{HBrO}_2 + \text{H}_2\text{O}$	$k_{19} = 1 \times 10^{-5} \text{ mol}^{-2} \text{ dm}^6 \text{ s}^{-1}$	

^a Values refer to temperature of 20 °C. $[\text{H}_2\text{O}] = 55 \text{ mol dm}^{-3}$ included in the rate constant. CHD = 1,4-cyclohexanedione; CHDE = enolized form of CHD; BrCHD = 2-bromo-1,4-cyclohexanedione, CHED = 2-cyclohexene-1,4-dione, H_2Q = 1,4-dihydroxybenzene; Q = 1,4-benzoquinone, HQ^* = semiquinone radical.

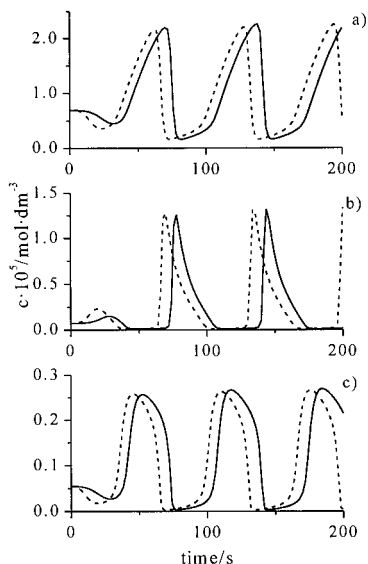
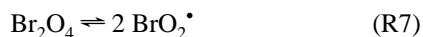
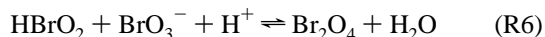


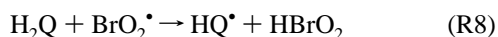
Figure 3. Simulated concentrations of (a) H_2Q , (b) HBrO_2 , and (c) Br^- . Initial concentrations are the same as in Figure 2. Solid lines correspond to the original model (28 reactions). Dashed lines are simulated by the reduced model (21 reactions).

The connection between equilibrium reactions R6 and R7 has been discussed by Turányi et al.⁵



They investigated the GTF mechanism of the Belousov–Zhabotinsky reaction⁶ and concluded that R7 and R-7 are fast equilibrium reactions.

Reduction of BrO_2^* by H_2Q is also an important reaction cluster.



Reaction R9 is diffusion controlled, and the HQ^* radical is considered to be a QSSA species.

TABLE 2. Reaction Importances at the Different Observation Time^a

	1	2	3	4	5	6	7	8	9	10	11	12	13	14	15	16
R1	⊗	⊗	⊗	⊗	⊗	⊗	⊗	⊗	⊗	⊗	⊗	⊗	⊗	⊗	⊗	⊗
R-1	⊗	⊗	⊗	⊗	⊗	⊗	⊗	⊗	⊗	⊗	⊗	⊗	⊗	⊗	⊗	⊗
R2	⊗	⊗	⊗	⊗	⊗	⊗	⊗	⊗	⊗	⊗	⊗	⊗	⊗	⊗	⊗	⊗
R-2																
R3					⊗	⊗					⊗	⊗	⊗			
R-3																
R4	⊗	⊗	⊗	⊗	⊗	⊗	⊗	⊗	⊗	⊗	⊗	⊗	⊗	⊗	⊗	⊗
R-4	⊗	⊗	⊗	⊗	⊗	⊗	⊗	⊗	⊗	⊗	⊗	⊗	⊗	⊗	⊗	⊗
R5								⊗								⊗
R6	⊗	⊗	⊗	⊗	⊗	⊗	⊗	⊗	⊗	⊗	⊗	⊗	⊗	⊗	⊗	⊗
R-6	⊗	⊗	⊗	⊗	⊗	⊗	⊗	⊗	⊗	⊗	⊗	⊗	⊗	⊗	⊗	⊗
R7	⊗	⊗	⊗	⊗	⊗	⊗	⊗	⊗	⊗	⊗	⊗	⊗	⊗	⊗	⊗	⊗
R-7	⊗	⊗	⊗	⊗	⊗	⊗	⊗	⊗	⊗	⊗	⊗	⊗	⊗	⊗	⊗	⊗
R8	⊗	⊗	⊗	⊗	⊗	⊗	⊗	⊗	⊗	⊗	⊗	⊗	⊗	⊗	⊗	⊗
R9	⊗	⊗	⊗	⊗	⊗	⊗	⊗	⊗	⊗	⊗	⊗	⊗	⊗	⊗	⊗	⊗
R10																
R-10																
R11	⊗	⊗	⊗	⊗	⊗	⊗	⊗	⊗	⊗	⊗	⊗	⊗	⊗	⊗	⊗	⊗
R-11	⊗	⊗	⊗	⊗	⊗	⊗	⊗	⊗	⊗	⊗	⊗	⊗	⊗	⊗	⊗	⊗
R12	⊗	⊗	⊗	⊗	⊗	⊗	⊗	⊗	⊗	⊗	⊗	⊗	⊗	⊗	⊗	⊗
R13								⊗	⊗							⊗
R14	⊗	⊗	⊗	⊗	⊗	⊗	⊗	⊗	⊗	⊗	⊗	⊗	⊗	⊗	⊗	⊗
R15	⊗	⊗	⊗	⊗	⊗	⊗	⊗	⊗	⊗	⊗	⊗	⊗	⊗	⊗	⊗	⊗
R16																
R17					⊗	⊗	⊗	⊗		⊗	⊗	⊗	⊗	⊗		⊗
R18																
R19	⊗	⊗	⊗	⊗	⊗	⊗	⊗	⊗	⊗	⊗	⊗	⊗	⊗	⊗	⊗	⊗

^a Symbols indicate the important reactions.

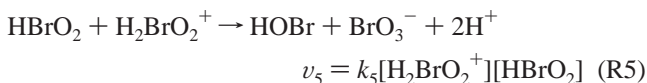
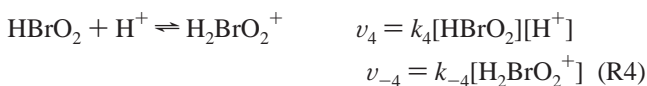
We can conclude that there are two main reaction groups in the mechanism. The first is the bromination of CHD and the formation of H_2Q and Br^- from BrCHD (R1, R2, R3, R11, R12, R13, R14, and R15). The second is the autocatalytic reaction of bromate and H_2Q (R6, R7, R8, R9, and R10).

We have identified those six reactions R-2, R-3, R10, R-10, R16, and R18 which are insignificant during the examined period of the reaction (Table 2). R-2 and R-3 also were found to be unimportant reactions in the analysis of the GTF mechanism of the BZ reaction.⁵ The high concentration of CHD means that Br_2 and HOBr are consumed more rapidly in R12 and R13 than in R16 and R18. 1,4-Benzoquinone is a reactant only in R-10 so it can be neglected. After the reduction, the model contains 14 species and 21 reactions and still reproduces the behavior of the original model (Figure 3).

Skeleton Models

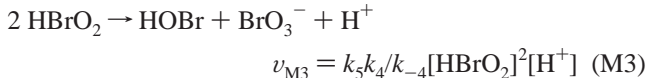
The aim of the simplification is the identification of the minimal set of reactions and components that still reproduces the limit-cycle oscillations. We regard Br^- , H_2Q , and HBrO_2 as the important species and therefore the skeleton model should reproduce the concentration changes of these components. We used pool-component approximation for species of high concentrations, i.e., for CHD, BrCHD, CHED, and bromate. The first step was the systematic elimination of the consumption and production reactions of all components with the exception of those reactions that contain the pool components and Br^- , H_2Q , and HBrO_2 . Thus we eliminated the consumption reactions of HOBr and Br_2 and the production reactions of Br_2 (R1, R-1, R12, and R13). The enolization equilibrium of CHD (R11 and R-11) and reaction R19 were also eliminated. The mechanism thus obtained can still reproduce the oscillations.

The next step was to apply QSSA for H_2BrO_2^+ and HQ^* . In the case of H_2BrO_2^+ :

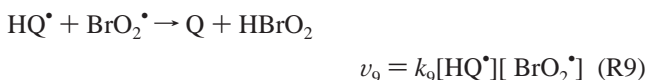
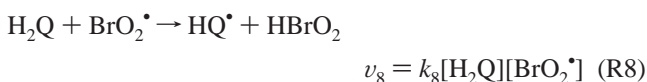


$$[\text{H}_2\text{BrO}_2^+]_{\text{QSSA}} = \frac{k_4[\text{HBrO}_2][\text{H}^+]}{k_4 + k_5[\text{HBrO}_2]} \approx \frac{k_4[\text{HBrO}_2][\text{H}^+]}{k_{-4}} \quad (\text{E1})$$

We could replace R4 and R5 by reaction M3:

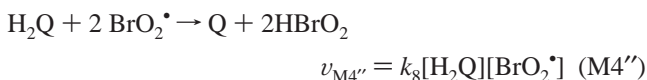


In the case of HQ^* :

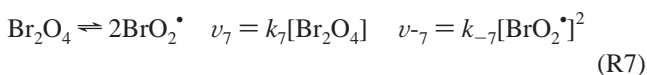
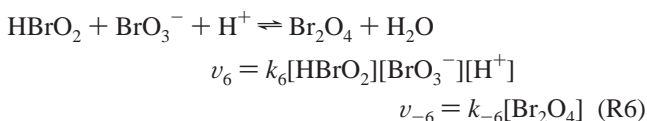


$$[\text{HQ}^*]_{\text{QSSA}} = \frac{k_8[\text{H}_2\text{Q}]}{k_9} \quad (\text{E2})$$

Reactions R8 and R9 are replaced by

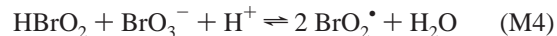


We used the approximation of Turányi et al.⁵ for Br_2O_4 .



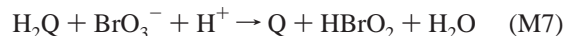
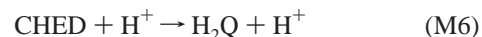
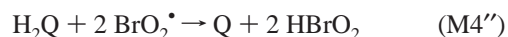
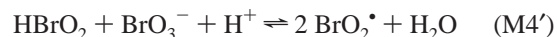
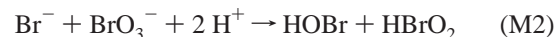
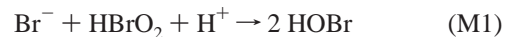
$$[\text{Br}_2\text{O}_4]_{\text{Eq}} = \frac{k_{-7}[\text{BrO}_2^*]^2}{k_7} \quad (\text{E3})$$

It allows us to replace reactions R6 and R7 by the following equilibrium reaction:



$$v_{\text{M4}'} = k_6[\text{HBrO}_2][\text{BrO}_3^-][\text{H}^+] \quad v_{\text{M4}''} = k_{-6}[\text{Br}_2\text{O}_4]_{\text{Eq}}$$

The result of the simplification is a four-variable model:

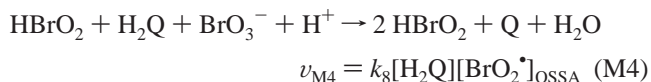


This is a purely mass-action kinetic skeleton model. Obviously according to the full component approximations it can not simulate the induction period. We have to estimate the concentrations of BrCHD and CHED for the simulation. We shall return to this point later. For further simplification we eliminated BrO_2^* by QSSA from the model.

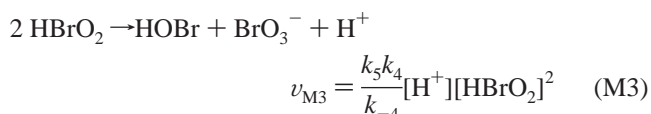
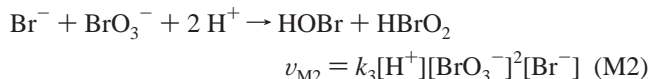
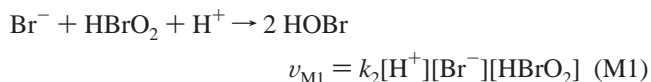
$$[\text{BrO}_2^*]_{\text{QSSA}} = \frac{k_7(-k_8[\text{H}_2\text{Q}] + W)}{2k_{-6}k_{-7}} \quad (\text{E4})$$

$$W = \sqrt{(k_8[\text{H}_2\text{Q}])^2 + 4 \frac{k_{-6}k_{-7}k_6}{k_7} [\text{HBrO}_2][\text{BrO}_3^-][\text{H}^+] } \quad (\text{E5})$$

Reactions M4' and M4'' are reduced to reaction M4:



In this way we get a simple three-variable model:

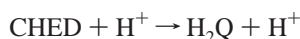




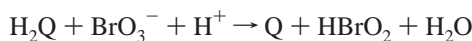
$$v_{M4} = k_8[\text{H}_2\text{Q}][\text{BrO}_2^*]_{\text{QSSA}} \quad (\text{M4})$$



$$v_{M5} = k_{14}[\text{H}^+][\text{BrCHD}] \quad (\text{M5})$$



$$v_{M6} = k_{15}[\text{H}^+][\text{CHED}] \quad (\text{M6})$$



$$v_{M7} = k_{17}[\text{H}^+][\text{BrO}_3^-][\text{H}_2\text{Q}] \quad (\text{M7})$$

These models reproduce the temporal, dynamical behavior of the original model (Figure 4). It is important to note that all of rate constants included in these models have been determined experimentally.

We can explain the oscillatory behavior of the reacting system by the three-variable model (Figure 5). The first part of the oscillation starts at point A and terminates at point B. At point A the concentrations of H_2Q , Br^- , and HBrO_2 are low, because the rate of Br^- production is faster than the rate of H_2Q production. Bromide ions reach the high steady-state concentration rapidly and win the competition for HBrO_2 (M1) over H_2Q (M4). The result is the slow accumulation of H_2Q . At point B (Figure 5) H_2Q concentration is high enough to trigger the autocatalytic reaction M4. However, it results in a rapid decrease in H_2Q concentration, and the autocatalysis is terminated at point C. After it reactions M1 and M3 slowly consume HBrO_2 and the system returns to state A.

Stability Analysis

For the stability analysis we made some further simplifications. We reduced M5 and M6 to reaction E and introduced a stoichiometric parameter f , which is the ratio of the rate of production of Br^- and H_2Q . The rate equation of the autocatalytic reaction has been modified, too. In this modification instead

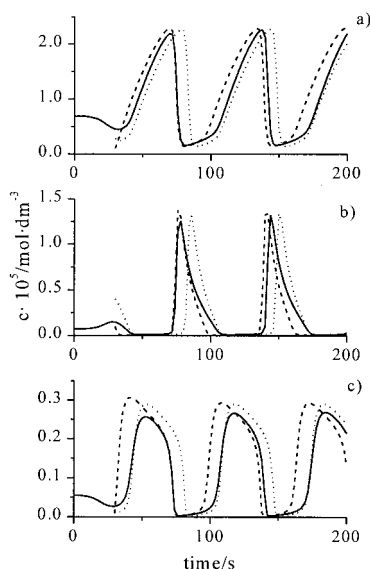


Figure 4. Comparison of the concentration changes of (a) H_2Q , (b) HBrO_2 , and (c) Br^- simulated by original model (solid lines), the four variable (dotted lines), and the three variable models (dashed lines). Initial concentrations are the same as in Figure 2.

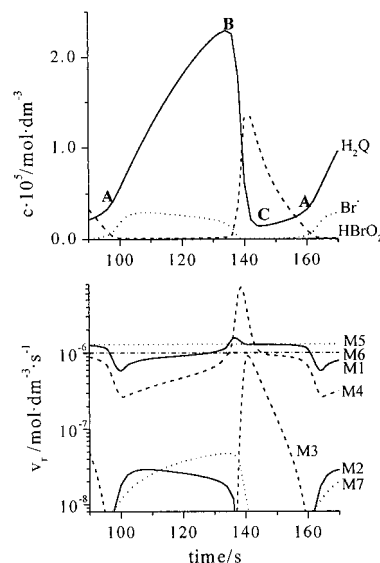
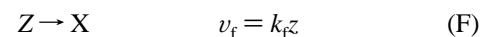
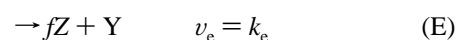
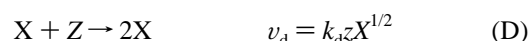
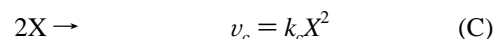
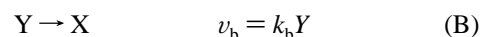
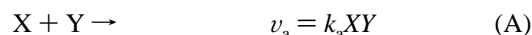


Figure 5. Concentration and reaction rate changes during an oscillation. Curves simulated by three variable model. Initial concentrations are the same as in Figure 2.

of QSSA we used the equilibrium concentration of BrO_2^* radical.



Where X = concentration of HBrO_2 , Y = concentration of Br^- , Z = concentration of H_2Q , $k_a = k_2[\text{H}^+]$, $k_b = k_3[\text{BrO}_3^-][\text{H}^+]^2$, $k_c = k_5 k_4 / k_{-4}[\text{H}^+]$, $k_e = k_{14}[\text{BrCHD}][\text{H}^+]$, $f = ([\text{CHED}])k_{15} / ([\text{BrCHD}]k_{14})$, $k_f = k_{17}[\text{BrO}_3^-][\text{H}^+]$, and $k_d = k'_d[\text{BrO}_3^-]^{1/2}[\text{H}^+]^{1/2}$. Using the equilibrium assumption for BrO_2^* radical, we get $k'_d = k_8((k_7 k_6) / k_7 k_6)^{1/2}$. The results from the simulation using k'_d were not good enough. However, if k'_d is considered as an adjustable parameter, the model could reproduce the behavior of the original model. The dimensionless equations of this system are

$$\frac{dx}{d\tau} = y(\beta - \alpha x) + z(\gamma x^{1/2} + 1) - \delta x^2 \quad (\text{E6})$$

$$\frac{dy}{d\tau} = 1 - y(\beta + \alpha x) \quad (\text{E7})$$

$$\frac{dz}{d\tau} = f - z(\gamma x^{1/2} + 1) \quad (\text{E8})$$

Let $\vartheta = \alpha/\beta$ and use QSSA for y ($y_{\text{QSSA}} = 1/(\alpha x + \beta)$). The result is a two-dimensional system:

$$\frac{dx}{d\tau} = \frac{(1 - \vartheta x)}{(1 + \vartheta x)} + z(\gamma x^{1/2} + 1) - \delta x^2 \equiv a(x, z) \quad (\text{E9})$$

$$\frac{dz}{d\tau} = f - z(\gamma x^{1/2} + 1) \equiv b(x, z) \quad (\text{E10})$$

We may conclude that there are two important parameters, μ

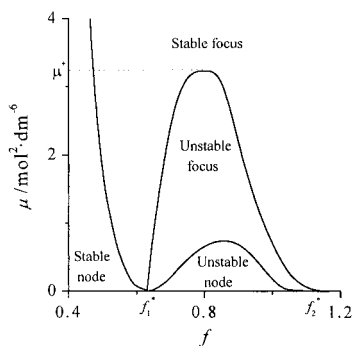


Figure 6. Calculated bifurcation diagram.

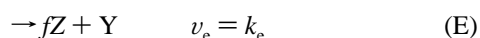
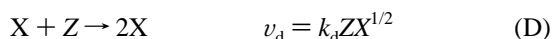
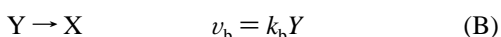
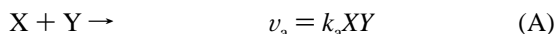
$= ([\text{BrO}_3^-]^2[\text{H}^+])/[\text{BrCHD}]$ (included in ϑ and γ) and f the ratio of the rate of production of H_2Q and Br^- . By numerical studies on the local stability of the stationary state we constructed a bifurcation diagram (Figure 6). We have found that a limit cycle behavior developed by Hopf bifurcation. Oscillations can occur in the system if $f_1^* < f < f_2^*$ and $\mu < \mu^*$ (where $f_1^* \approx 0.63$, $f_2^* \approx 1.1$, and $\mu^* \approx 3.3 \text{ mol}^2 \text{ dm}^{-6}$). The corresponding chemical conditions are the following:

$$0.63v_{\text{prod}}^{\text{Br}} \leq v_{\text{prod}}^{\text{H}_2\text{Q}} \leq 1.1v_{\text{prod}}^{\text{Br}} \quad \text{and} \quad [\text{BrO}_3^-]^2[\text{H}^+] < 3.3[\text{BrCHD}]$$

The first means that the rate of H_2Q production has to be only slightly lower than the rate of the production of bromide ions. The second means that the production of H_2Q and bromide ions (reaction E) has to be fast enough comparable with the production of bromous acid in reaction of bromide and bromate (B). It is important to note that the fast removal of bromine by CHD is another essential condition for the oscillation. These conditions allow us to estimate the concentrations of CHED and BrCHD that are necessary for simulation by the reduced models.

It is worth to study the nullclines ($a(x,z)=0$, $b(x,z)=0$) of the system. The z -nullcline is a monotone curve and depends on parameters f and γ . The x -nullcline depends on parameters ϑ , γ and δ and it has a maximum at low x values ($x < 10^{-2}$). When oscillations occur in the system than the intersection is to the right from the maximum of x -nullcline (Figure 7). The position of the intersection at constant μ depends on the f parameter. At $f = f_1^*$, the intersection is in the maximum of the x -nullcline.

The mechanistic analysis revealed that reactions C and F have minor importance.



By using QSSA for Y and the dimensionless forms the result is a simple two variable system:

$$\frac{dx}{d\tau} = \gamma x^{1/2} \underline{z} - \frac{\vartheta x - 1}{\vartheta x + 1} \quad (\text{E11})$$

$$\frac{dz}{d\tau} = f - \gamma x^{1/2} \underline{z} \quad (\text{E12})$$

We have only three parameters, and two of them (γ and ϑ)

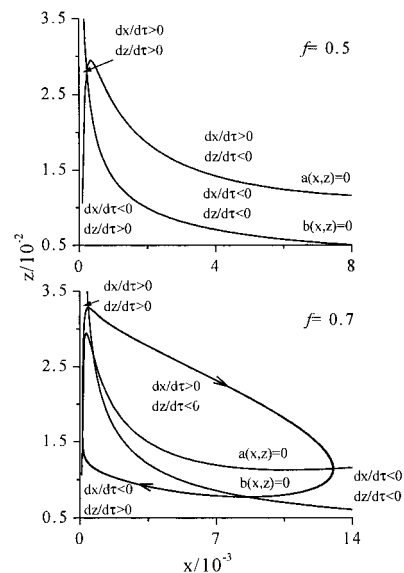


Figure 7. Phase-space at $\mu = 0.4 \text{ mol}^2 \text{ dm}^{-6}$. At $f = 0.5$ the stationary state is stable. At $f = 0.7$ the stationary state is unstable.

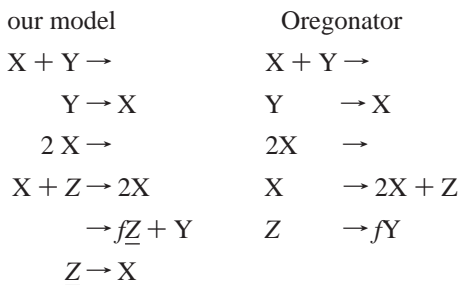
depend on μ . By examining these three parameters we can calculate analytically the critical values of the f parameter (see Appendix):

$$f_1^* = \frac{1}{2}(\sqrt{5} - 1), \quad f_2^* = 1$$

Discussion

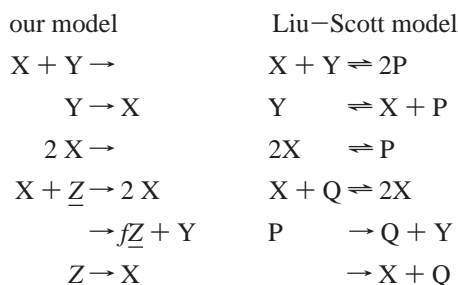
The CHD–bromate–acid reacting system, although similar in some characteristics to other bromate-driven oscillators, exhibits some of unique features. As we pointed out in our previous paper,² its oscillatory behavior can be attributed to an intermediate rather stable oxidation product of CHD. It is the H_2Q that is generated continuously and is one of the components of a clock-type reaction, a composite process of the chemical oscillator.

Let us compare our model [reactions A–F] with the well-known, five-step Oregonator. In the Oregonator model, the control intermediate, the bromide ion, is generated, in a rather sophisticated series of reactions, by the oxidized form of the catalyst, $\text{Z} \rightarrow \text{Y}$, (where Z stands for, e.g., Ce^{4+} or Mn^{3+}). A striking difference is that our model does not contain a corresponding reaction. In our uncatalyzed bromate oscillator (UBO), the product of the organic is Q (1,4-benzoquinone) which, however, does not participate in further redox reactions, thus it cannot generate bromide ions. The analysis of the mechanism reported in our previous paper points to the fact that in the control of oscillations besides bromide ion H_2Q is also involved. During the slow bromide-ion consumption phase (in the first kinetic state of the FKN mechanism⁷), H_2Q is accumulated and when $[\text{Br}^-]$ drops below the critical value and $[\text{H}_2\text{Q}]$ reaches a threshold value the autocatalytic reaction is initiated. The termination of the autocatalysis can be attributed to the drop of $[\text{H}_2\text{Q}]$ below a critical level. We may conclude that the fifth reaction in our model, the production of both bromide ion and H_2Q , is responsible for the chemical control. This system is somewhat similar to a reaction proceeding in a continuously fed reactor (or to a semibatch system).



where $X = \text{HBrO}_2$, $Y = \text{Br}^-$, $Z = \text{H}_2\text{Q}$, $Z = \text{Ce}^{4+}$.

A somewhat similar model has been suggested by Liu and Scott⁸ who examined the behavior of an UBO in CSTR. Their model successfully simulated the observed experimental responses. The main characteristics of their model are the following: (1) bromide ion is formed in the reaction of bromate and the starting aromatic and (2) in the same reaction a quinone derivative is formed which catalyzes the bromate–bromous acid reaction.



where $P = \text{HOBr}$ and $Q = \text{quinone}$. In the Liu–Scott model, HOBr plays an important role; brominated intermediates, however, are not considered as sources for bromide ions. Györgyi et al.⁹ have reported that certain aromatics are brominated in very fast reactions, and bromine, respectively HOBr are consumed immediately and therefore they can not participate in the production of bromide ions. A similar situation exists in the CHD–bromate–acid system.

Considering the mechanism of the CHD–bromate reacting system, it can be concluded that it is closely related to many CSTR oscillators. Most CSTR oscillators are not self-contained; that is, they do not oscillate without the CSTR flow. They are “emptying/refilling” oscillators. The reactor fills with some substrate until eventually an autocatalytic reaction is triggered, which rapidly consumes essentially all of that substrate. The system is then quiescent while being reinitialized and refilled with another pulse.

Our analysis shows that this is indeed the case in the CHD–bromate oscillator. The autocatalytic substrate is H_2Q that is steadily produced by the oxidation of CHD by bromate. It thus accumulates until eventually suddenly and autocatalytically oxidized to Q by bromate. The system is then quiescent until sufficient H_2Q accumulates for another pulse. Bromide ion does not appear to be dynamically critical to the appearance of oscillations, although it may well mediate the system quantitatively.

Notwithstanding that the CHD–bromate system is a bromate-driven oscillator, it is dynamically quite different from classic system represented by the Oregonator.

Acknowledgment. This work was supported by the Hungarian Scientific Research Fund (Grant OTKA Nos. T 016680 and F 017073).

Appendix

Dimensionless Forms. When we let $x = k_f/k_e X$, $y = k_f/k_e Y$, $z = k_f/k_e Z$, and $\tau = k_f t$, eqs E6–E8 emerge with the following dimensionless parameters:

$$\alpha = k_a k_e / k_f^2 = \frac{k_2 k_{14} [\text{BrCHD}]}{k_{17}^2 [\text{BrO}_3^-]^2}$$

$$\beta = k_b / k_f = k_3 / k_{17} [\text{H}^+]$$

$$\gamma = k_d k_e^{1/2} / k_f^{3/2} = \frac{k'_d k_{14}^{1/2} [\text{BrCHD}]^{1/2}}{k_{17}^{3/2} [\text{H}^+]^{1/2} [\text{BrO}_3^-]}$$

$$\delta = 2 \frac{k_c k_e}{k_f^2} = 2 \frac{k_5 k_4 k_{14} [\text{BrCHD}]}{k_{-4} k_{17}^2 [\text{BrO}_3^-]^2}$$

For $[\text{NaBrO}_3]_0 = 0.08 \text{ mol dm}^{-3}$, $[\text{BrCHD}]_0 = 0.02 \text{ mol dm}^{-3}$, $[\text{CHED}]_0 = 0.004 \text{ mol dm}^{-3}$, $[\text{H}^+]_0 = 1.29 \text{ mol dm}^{-3}$, and $k'_d = 280 \text{ mol}^{-3/2} \text{ dm}^{9/2} \text{ s}^{-1}$, we obtain $\alpha = 10^6$, $\beta = 77.4$, $\gamma = 1102$, $\delta = 2719$, $f = 0.776$.

By using $\mu = [\text{BrO}_3^-]^2 [\text{H}^+] / [\text{BrCHD}]$, we get the next following formulas:

$$\vartheta = \frac{\alpha}{\beta} = \frac{k_2 k_{14}}{k_3 k_{17}} \mu^{-1}$$

$$\gamma = \frac{k'_d k_{14}^{1/2}}{k_{17}^{3/2}} \mu^{-1/2}$$

Local Stability of the Stationary States. The first step is to find the stationary solutions:

$$z_s = f / \gamma x_s^{1/2} \quad (\text{E13})$$

$$x_s = f + 1 / \vartheta (1 - f) \quad (\text{E14})$$

To study the stability of the stationary states, we have to examine the determinant and the trace of the jacobian of the system:

$$\text{Det}(J)_s = \frac{2\gamma\vartheta x_s^{1/2}}{(\vartheta x_s + 1)^2} \quad (\text{E15})$$

$$\text{trace}(J)_s = \frac{\gamma(z_s - 2x_s)}{2x_s^{1/2}} - \frac{2\vartheta}{(\vartheta x_s + 1)^2} \quad (\text{E16})$$

The determinant is always positive so the condition for the Hopf bifurcation is

$$\text{trace}(J)_s = 0 \quad (\text{E17})$$

$$-\frac{(f^3 - 2f + 1)(1 - f)^{1/2}}{2(f + 1)^{3/2}} = \frac{k'_d (k_3)^{3/2}}{k_{14} (k_2)} \mu \quad (\text{E18})$$

To find the critical f values we have to solve eq 11 at $\mu = 0$

$$(f^3 - 2f + 1)(1 - f)^{1/2} = 0 \quad (\text{E19})$$

The results are (the negative is not relevant)

$$f_1^* = \frac{1}{2}(\sqrt{5} - 1) \quad f_2^* = 1 \quad f_3 = -\frac{1}{2}(\sqrt{5} - 1)$$

References and Notes

- (1) Kurin-Csörgei, K.; Szalai, I.; Molnár-Perl, I.; Körös, E. *React. Kinet. Lett.* **1994**, *53*, 115. Molnár-Perl, I.; Tisza, S.; Körös, E.; Kurin-Csörgei,

- K.; Szalai, I. *J. High Resolut. Chromatogr.* **1995**, 18, 749. Kurin-Csörgei, K.; Szalai, I.; Körös, E. *React. Kinet. Lett.* **1995**, 54, 217.
- (2) Szalai, I.; Körös, E. *J. Phys. Chem.* **1998**, 102, 6892.
- (3) Edblom, E. C.; Orbán, M.; Epstein, I. R. *J. Am. Chem. Soc.* **1986**, 108, 2826. Edblom, E. C.; Györgyi, L.; Orbán, M.; Epstein, I. R. *J. Am. Chem. Soc.* **1987**, 109, 4876.
- (4) Turányi, T.; Bérces, T.; Vajda, S. *Int. J. Chem. Kinet.* **1989**, 21, 83. Turányi, T. *New J. Chem.* **1990**, 14, 795. Turányi, T. *J. Math. Chem.* **1990**, 5, 203.

- (5) Turányi, T.; Györgyi, L.; Field, R. J. *J. Phys. Chem.* **1993**, 97, 1931.
- (6) Györgyi, L.; Turányi, T.; Field, R. J. *J. Phys. Chem.* **1990**, 94, 7162.
- (7) Noyes, R. M.; Field, R. J.; Körös, E. *J. Am. Chem. Soc.* **1972**, 94, 1394.
- (8) Liu, J.; Scott, S. K. *J. Chem. Soc., Faraday Trans.* **1992**, 88, 909.
- (9) Györgyi, L.; Varga, M.; Körös, E.; Field, R. J.; Ruoff, P. *J. Phys. Chem.* **1989**, 93, 2836.